Front. Optoelectron. 2015, 8(3): 241–251
DOI 10.1007/s12200-015-0524-9

REVIEW ARTICLE

Recent progress in colloidal quantum dot photovoltaics

Xihua WANG (✉)

Department of Electrical and Computer Engineering, University of Alberta, Edmonton, Alberta T6G 2V4, Canada

Abstract The development of photovoltaic devices, solar cells, plays a key role in renewable energy sources. Semiconductor colloidal quantum dots (CQDs), including lead chacolgenide CQDs that have tunable electronic bandgaps from infrared to visible, serve as good candidates to harvest the broad spectrum of sunlight. CQDs can be processed from solution, allowing them to be deposited in a roll-to-roll printing process compatible with low-cost fabrication of large area solar panels. Enhanced multi-exciton generation process in CQD, compared with bulk semiconductors, enables the potential of exceeding Shockley-Queisser limit in CQD photovoltaics. For these advantages, CQDs photovoltaics attract great attention in academics, and extensive research works accelerate the development of CQD based solar cells. The record efficiency of CQD solar cells increased from 5.1% in 2011 to 9.9% in 2015. The improvement relies on optimized material processing, device architecture and various efforts to improve carrier collection efficiency. In this review, we have summarized the progress of CQD photovoltaics in year 2012 and after. Here we focused on the theoretical and experimental works that improve the understanding of the device physics in CQD solar cells, which may guide the development of CQD photovoltaics within the research community.

Keywords colloidal quantum dot (CQD), solar cell, photovoltaics, carrier extraction, light trapping

1 Introduction

Colloidal quantum dot (CQD) semiconductors are quantum materials, in which the bandgap can be tuned by altering the size of quantum dots. In 1983, Brus et al. reported the first CQD synthesis by aqueous and ionic chemistry [1]. In 1993, Bawendi et al. reported nearly monodispersed CQD materials using hot-injection method [2]. Since then, CQD materials and devices attract great attention in academics and industries, and show broad applications from biology to optoelectronics. In the research of CQD optoelectronics, CQD materials have been demonstrated to make light-emitting diodes (LEDs), solar cells, and photodetectors. The development of CQD LEDs can be found in a recent review [3]. A comprehensive review of CQD photodetectors is available in Ref. [4].

CQD photovoltaics are of great interest in academic and industry, and have shown rapid progress recently. This journal published a review on the development of CQD photovoltaics in year 2011 – 2012. Thus, the scope of this article is to summarize research works of CQD photovoltaics in year 2012 and after. There are several review papers on CQD photovoltaics in the past two years. Readers can obtain the comprehensive view on the development of CQD solar cells in Refs. [5,6]. Reviews from the perspective of device architectures can be found in Refs. [7,8]. To distinguish from other reviews, this paper focuses on the theoretical and experimental works that improve the understanding of device physics in CQD solar cells and improved device performance following these principles.

In this review, Section 2 will cover the fundamentals of generation, recombination and charge transport in p-n junction solar cells. In Section 3, the development of high quality CQD films for photovoltaics will be discussed. Section 4 will focus on light trapping techniques for light absorption enhancement in CQD films. Section 5 will include recent progress in material processing and device fabrication for cost-effective CQD solar cell manufacturing. In the end, some prospective comments will be addressed.

2 Fundamentals of generation, recombination and charge transport in p-n junction solar cells

Photovoltaic devices, solar cells, can efficiently utilize solar energy by converting it directly to electricity using organic or inorganic semiconductor materials. Nowadays,

Received April 13, 2015; accepted June 19, 2015

E-mail: xihua@ualberta.ca

the materials in high-performance CQD solar cells are PbS and PbSe, and the dominant device architecture in single-junction PbS CQD solar cells is p-n junction.

In p-n junction solar cells, an electron-hole pair is excited after an incident photon is absorbed. Usually, electron-hole pairs can easily dissociate to free electrons and holes in inorganic semiconductors due to the low coulomb binding energy. These free electrons and holes are collected at the electrodes before they are recombined. CQD materials have relative low absorption coefficient ($\sim 10^4\,\mathrm{cm}^{-1}$) at their band edges. Thus, several microns thick CQD films are required to achieve $> 90\%$ light absorption. However, current CQD solar cells have an optimum thickness of ~300 nm [7]. To solve this challenge, researchers work on two approaches: 1) various methods to suppress recombination for increasing optimum thickness, which will be discussed in Section 3; 2) light trapping techniques for enhancing light absorption in CQD thin films, which will be discussed in Section 4.

In solar cells, the figure of merit is current-voltage (*I-V*) characteristics. In this measurement, a bias voltage is applied to the two terminal of an illuminated solar cell, and the current passing through the devices is probed. The current at zero bias voltage is called short circuit current, I_{sc}. The bias voltage at zero current is called open circuit voltage, V_{oc}. The device achieves the maximum photon-to-electricity conversion at the maximum power point, where the value of current times voltage reaches the maximum. At this condition, the ratio of the power of generated electricity over the power of incident light represents the power conversion efficiency (PCE) of the solar cell. The device modeling of p-n junction solar cells is built on five equations [9]: two current equations, one Poisson's equation, and two continuity equations. The following parameters with extracted values from experiments are required for quantitative device modeling: electron and hole mobilities, dopant density, band-to-band recombination coefficient, semiconductor electronic band structure, and electrical properties (such as energy levels, densities, capture cross-sections etc.) of traps. Through simulation, we can obtain the electric potential, electric field, electron density, hole density, electron current, hole current, generation rate and recombination rate at any position in the device. The difference of electric potentials between the two terminals is the applied bias. The sum of electron current and hole current at the two terminals is the probed current. It is noted that the sum of electron current and hole current is not constant through the device due to different generation and recombination rates at different locations.

The optimum thickness of CQD films can be predicted using device modeling if all these parameters can be accurately extracted from experiments. However, all of the quantitative values of these parameters have not been identified in CQD solar cells. Considering that the device physics of CQD solar cells is still not fully clear, it is not possible to assign accurate values for all parameters. For example, theoretical works [10] suggest that the formation or breaking of atomic dimers at the PbS and CdSe CQD surface is the physic's origin of traps close to conduction band, but there is no direct evidence from experiments.

Fortunately, after several years' development in CQD photovoltaics, there is a simplified picture to describe the device physics in a p-n junction solar cell with the p-type CQD film. The density of photo-generated free electrons and holes are low compared to the dopant density. This is considered as low-level injection in semiconductors, thus only the carrier lifetime of electrons is of interest. In low-injection, Auger recombination can be ignored, therefore free electrons can only recombine with holes either through band-to-band transition, or through trap-assisted recombination (Shockley-Read-Hall process). In band-to-band transition, the carrier lifetime for electrons is

$$\tau_{b-b} = \frac{1}{R_{ec} N_A}.$$

PbS CQDs are direct bandgap materials, R_{ec} is the recombination coefficient and is about $10^{-10}\,\mathrm{cm}^3/\mathrm{s}$ for direct-bandgap semiconductors, so τ_{b-b} is in the order of microseconds for moderate doping ($N_A \sim 10^{16}\,\mathrm{cm}^{-3}$). The trap-assisted recombination is the process combining electron capture and hole capture, so only those traps near the mid-gap [11] are effective recombination centers. The electron lifetime, τ_{trap}, depends on the energy levels, densities, and capture cross-sections of trap states. Although it is unknown in CQD films, it is estimated to be much smaller than τ_{b-b} in CQD solar cells.

The charge transport in CQD solar cells should be discussed in two regions: space-charge (depletion) and charge neutral regions. The charge transport in the depletion region is a drift process, so the transient time of electrons, $t_{depletion}$, through the depletion region is determined by the drift velocity. The charge transport in charge neutral regions is a diffusion process, so the transient time, $t_{neutral}$, of electrons through charge neutral regions depends on the diffusivity. Both drift velocity and diffusivity are related to mobility of charge carriers. Higher electron mobility indicates that electrons can pass through depletion region and charge neutral regions faster, which leads to smaller transient times in both regions.

The overall collection efficiency of photo-generated charge carriers in CQD solar cells depends on the competition between charge transport and recombination. If τ_{trap} is much larger than $t_{depletion}$, most of the free electrons and holes generated in the depletion region of p-n junction solar cells can be collected by the electrodes. If τ_{trap} is much larger than $t_{neutral}$, most of the free electrons and holes generated in the charge neutral region can be collected by the electrodes. When the electron mobility approaches $\sim 10^{-2}\,\mathrm{cm}^2 \cdot \mathrm{V}^{-1} \cdot \mathrm{s}^{-1}$, the value of $t_{depletion}$ is in the order of nanoseconds. Higher electron mobility will reduce $t_{depletion}$ for faster charge transport in the depletion

region, so the chance of recombination in the depletion region may be small in CQD solar cells. Therefore, the major loss of photo-generated carriers is from the competition between τ_{trap} and $t_{neutral}$.

3 Recent development of CQD solar cells

Motivated by the above device physics, various recent works have been reported on improving carrier mobility and suppressing recombination. Other works, such as using n-type CQD and band engineering within CQD films to increase depletion region, also help to increase the optimum CQD film thickness.

3.1 Development of high mobility CQD films

As stated in Section 2, larger mobility means smaller $t_{depletion}$ and $t_{neutral}$, and higher power conversion efficiency (PCE) in CQD solar cells. Therefore, producing high mobility CQD film is the priority in the development of CQD solar cells. There have been several reports of electron mobility above 1 $cm^2 \cdot V^{-1} \cdot s^{-1}$ through field-effect transistor (FET) measurements [12,13]. However, none of these materials lead to champion devices in CQD photovoltaics. It is possible that the electrical properties of CQD films are highly sensitive to material processing. Material processing methods used to increase carrier mobility may reduce the carrier lifetime at the same time. The observed high gate-dependent carrier diffusion length [14] in FET measurement indicates a high density of mid-gap traps, which leads to short carrier lifetime. These CQD films leading to high performance solar cells, as shown in Fig. 1, only showed modest mobility [15–17] of ~10^{-3} to 10^{-2} $cm^2 \cdot V^{-1} \cdot s^{-1}$, and were characterized by time-of-flight or field-effect-transistor measurements. Thus, achieving high mobility while keep low density of mid-gap traps is critical in developing high performance CQD solar cells. High mobility alone, confirmed by FET measurements, does not assure high performance CQD solar cells.

3.2 Characterization of mid-gap traps

Although the depletion region could be large at equilibrium, the depletion region of solar cells operated at the maximum power point (MPP) is smaller due to the nonzero bias voltage. The PCE of solar cells is calculated when solar cells are operated at MPP. So high collection efficiency of carrier in charge neutral region is the key to achieve high performance for CQD solar cells. As discussed in Section 2, the competition between τ_{trap} and $t_{neutral}$ determines the collection efficiency of carrier. Recombination via mid-gap traps is a non-radiative process, however, this process may be characterized by the transient photoluminescence (PL) measurement, which probes the population of electrons in the conduction band. Since τ_{b-b} is much larger than τ_{trap}, the measured carrier lifetime can be considered to be τ_{trap}. The diffusion process in semiconductors is usually characterized by the diffusion length, $L_{diffusion} = \sqrt{D\tau}$, where $D = \left(\frac{kT}{q}\right)\mu$ and τ is the carrier lifetime. The PL quenching measurement is an effective approach to directly measure the carrier diffusion length [18]. Both techniques are simultaneously used to extract the carrier mobility in CQD films. Based on the above discussion, the optimum thickness of CQD film thickness should be the sum of depletion region at MPP and a thickness of ~$L_{diffusion}$.

In the past three years, various methods have been used to characterize the diffusion length and mid-gap traps. Zhitomirsky et al. measured the diffusion length of CQD solar cells [19] with 7% PCE using two approaches: devices with 1D and 3D structures. Both methods gave similar values for the diffusion length, 60 nm to 80 nm. They also reported the mobility of ~10^{-2} $cm^2 \cdot V^{-1} \cdot s^{-1}$ and the trap density of ~10^{16} cm^3 in the CQD films. Kemp et al. reported a diffusion length of 39 to 86 nm in CQD solar cell by analyzing the photocurrent extraction efficiency [20]. The mid-gap trap density measured by open-circuit transient decay method showed the value of ~2×10^{16} cm^3 in CQD films [15]. A more reliable estimation of diffusion length in CQD films was done by analyzing *I-V* characteristics in CQD solar cells [21] through a systematic measurement that was carried out on devices with different thickness. The diffusion length of ~150 nm was estimated from the trends of measured FF, J_{sc} and PCE values. As shown in Fig. 2, the diffusion length is about the thickness of charge neutral region of optimized solar cells operated at MPP.

For the first time, Carey et al. identified the physical origin of a trap state in CQD solar cells by theoretical and experimental studies [22]. They showed that ligand exchange unintended introduced a high molecular weight complex, containing both lead oleate and the shorter conductive ligand, and this poorly soluble complex could end up embedded within the CQD active layer and served as traps. Adding an acidic treatment during film processing could eliminate the complex and led to better device performance. However, this discovered trap is unlikely to be a mid-gap trap from its electroluminescence.

3.3 n-type CQD films and p-i-n devices

Before Tang et al. reported the first p-n homojection CQD solar cell [23] with n-type PbS CQD films in 2012, PbS and PbSe CQD films showed p-type semiconductor properties. The p-type behavior comes from ligands used in solid-state ligand exchange and oxidation by oxygen and water vapor. The homojunction CQD solar cells bypass the limit of narrow selection of electron-accepting layer in CQD solar cells, and may also help to reduce

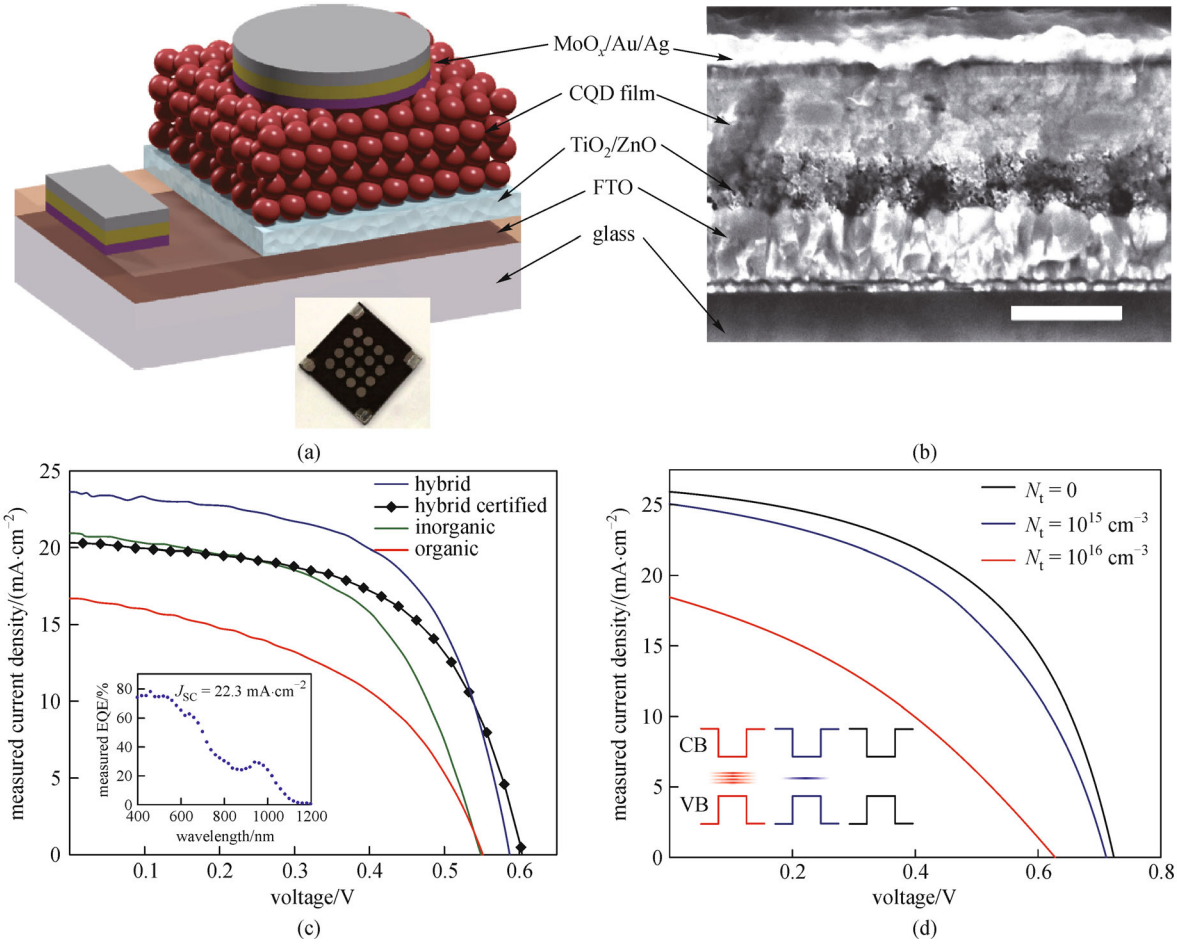

Fig. 1 Performance of CQD photovoltaics as a function of passivation (reprinted from Ref. [15])

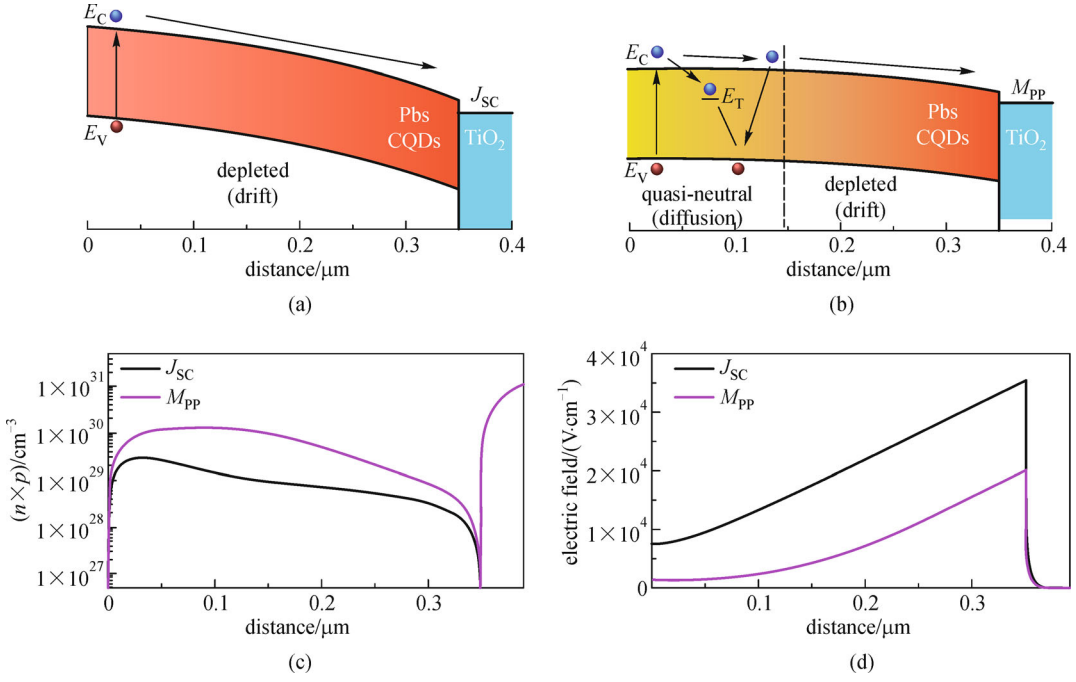

Fig. 2 Model and charge transport in CQD photovotlaics (reprinted from Ref. [21])

interface recombination [24] between electron-accepting layer and p-type CQD film. Various theoretical and experimental works [25,26] revealed the physical origin of n-type behavior in CQD films. The overall stoichiometry of the CQD, which can be altered by using different types of surface ligands, determines whether it is n-type or p-type.

Recent report [27,28] on air-stable n-type CQD solids employed inorganic passivants strongly binding to the CQD surface to repel oxidative attack. Air-stable devices were fabricated, and showed a PCE over 8% using inverted quantum junction architecture, as shown in Fig. 3. The doping level of middle n-type CQD film is very low, so its architecture is close to a p-i-n junction. Ko et al. also reported p-i-n heterojunction CQD solar cells [29] using non-CQD materials as n- and p-type layers.

3.4 Band engineering in CQD absorbing layers

It is well known that the bandgap of CQD films is influenced by the size of individual quantum dots and the coupling between quantum dots. Other electrical properties of CQD films, such as electron affinity and doping level of CQD films, can also be tuned by synthesis and surface ligands. This opens the possibility to add graded electrical properties in CQD absorbing layers. When combine two types of CQD films with different electron affinities, it may offer a favored band offset to block electron flow to the anode while facilitating hole extraction. When use two types of CQD films with different doping levels, it will form a depletion region at the adjacent region that extends the overall depletion width in solar cells. Therefore improve the carrier collection efficiency. Chuang et al. observed the modification of electron affinity in CQD films [30], and applied CQD films with different electron affinities to realize favored band bending in CQD films (Fig. 4). They reported a certified efficiency of 8.55% in their CQD solar cells. Ning et al. used CQD films with graded doping levels to achieve favored band bending in CQD films [31]. Their devices showed a PCE of 7.4%. Yuan et al. realized the graded doping levels in CQD films through molecularly engineering surface ligand coordination [32], and achieved a PCE over 7% in their devices.

4 Enhanced light absorption in CQD films using light trapping techniques

The low carrier diffusion length limits the optimum thickness of CQD films to be ~300 nm in solar cells. This thickness is far away from the optimum thickness for complete light absorption and leaves many of the incident

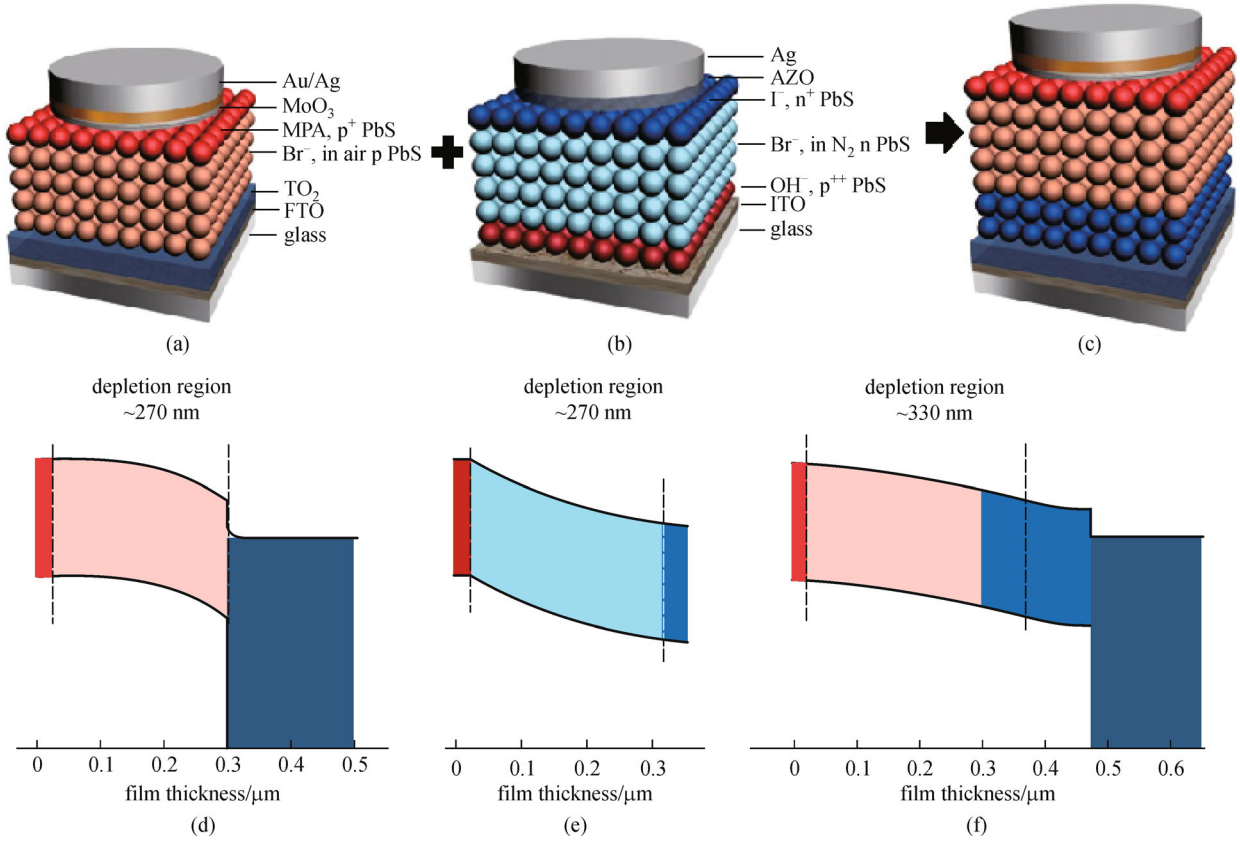

Fig. 3 Inverted quantum junction devices leverage process-compatible n- and p-type CQD solids (reprinted from Ref. [27])

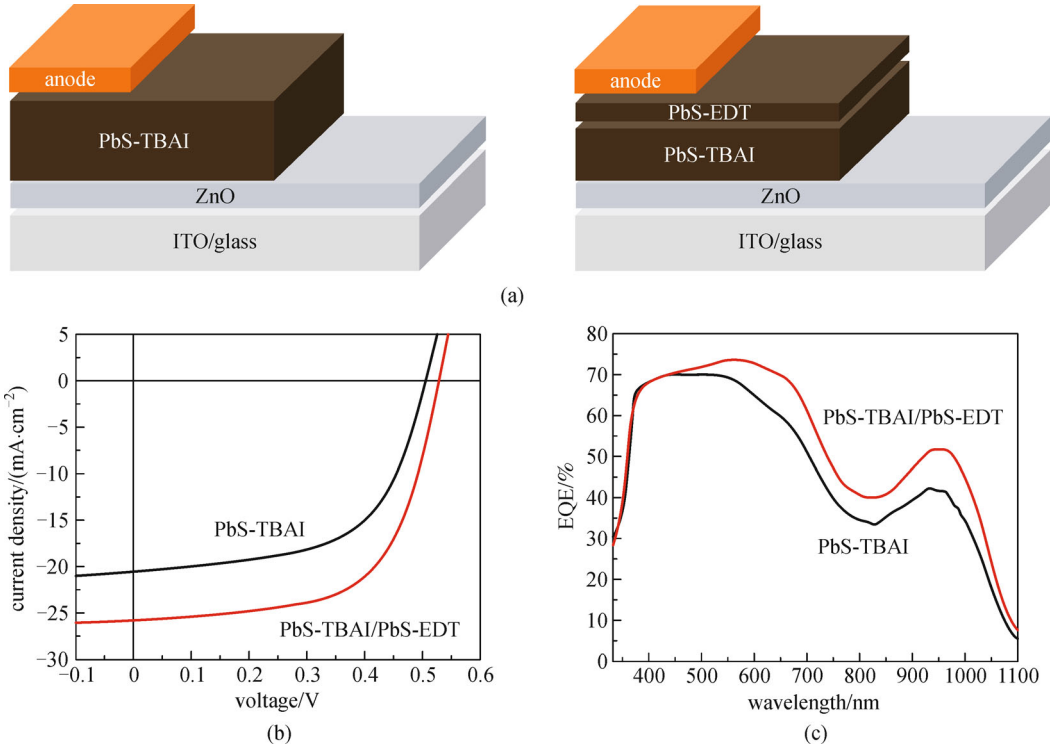

Fig. 4 Photovoltaic device architectures and performance (reprinted from Ref. [30])

photons uncollected. In addition to improve CQD film quality, another way to overcome the above-mentioned limitation is to increase the chance of light absorption inside the active layer by increasing the optical path length of incident light inside solar cell without increasing the thickness of the light absorbing layer. This is usually referred as the light trapping technique [33].

Early works using nanostructures were built on the empirical statement that hole diffusion length was larger than electron diffusion length in p-type CQD films. So nanostructured electron collection layer at the p-n junction interface could help to collect electrons in thick p-type CQD films. Kramer et al. reported ordered nanopillar structured electrodes for CQD solar cells [34]. Lan et al. demonstrated 7.3% CQD solar cells using ZnO/TiO_2 nanowire networks [35]. Since transparent conductive electrodes (TCOs) have different refractive index, compared with CQD films, there may be some scattering related light absorption enhancement in CQD film, but it is not analyzed and discussed in these references.

4.1 Light trapping by dielectric nanostructures

Periodic dielectric nanostructures have shown great potential for light trapping in various types of thin-film solar cells. In these devices, at least one dimension of structures is in the nanoscale and comparable to $\lambda/2n$, where λ is the wavelength of interest and n is the refractive index of dielectric material. Upon light trapping, the incident light is converted to optical resonance inside CQD films and analysis is done via wave optics theory. Adachi et al. reported a broadband absorption enhancement in CQD solar cells [36] using periodic nanostructured electrodes. The patterning of nanostructures was realized using nanosphere lithography, as shown in Fig. 5. Then the nanostructured electrode was covered by a semi-conformal PbS layer by dip-coating. An improvement of 31% in J_{sc} was observed due to the enhanced light absorption. However, due to reduced FF, the PCE was only increased from 5.3% for the planar device to 6.0% for nanostructured device. The finite-difference time-domain (FDTD) analysis showed optical resonance existing in CQD films. Mahpeykar et al. investigated the resonant coupling in CQD films using FDTD simulation [37]. They reported the influence of various shapes of nanostructured electrodes on the performance of light absorption enhancement, and proposed a 2D nanobranch array, which was able to maintain its performance despite structural imperfections common in fabrication. Mihi et al. reported the coupling of resonant modes using embedded dielectric microsphere in CQD solar cells [38]. They observed enhanced photocurrent, and attempted to maximize the number of resonant modes by locating microsphere at three different locations. Other reports used nanoimprinting to fabricate nanostructured electrodes [39,40], and observed enhanced light absorption and higher PCE values.

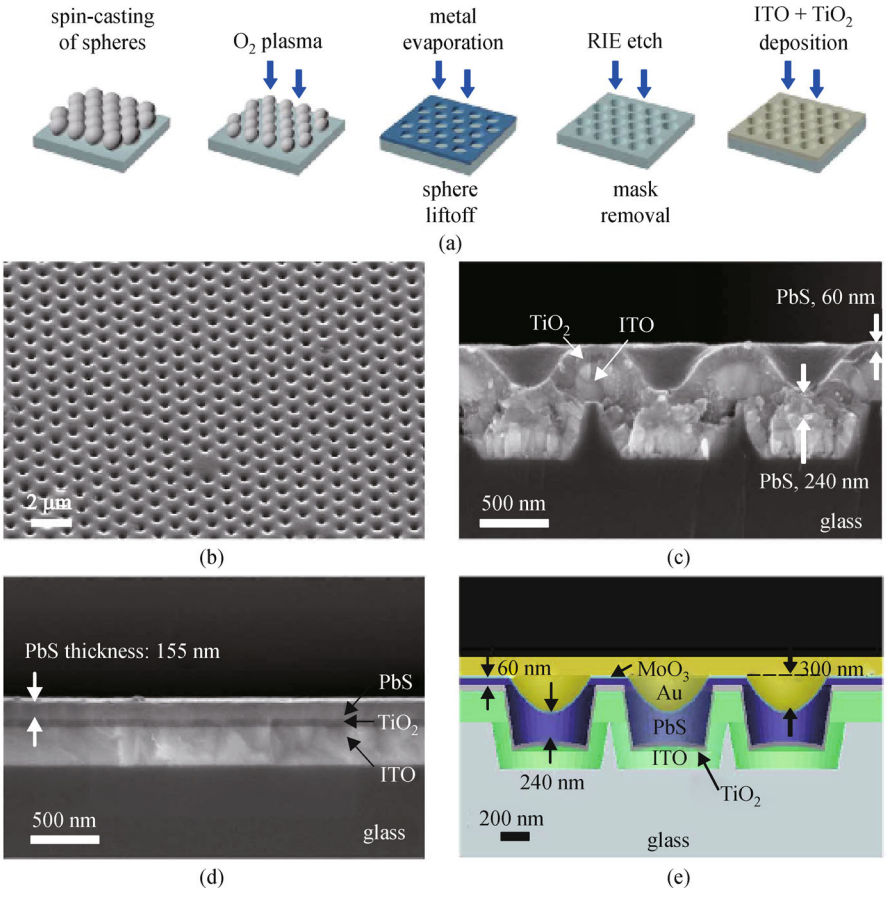

Fig. 5 Fabricated nanostructured CQD solar cells (reprinted from Ref. [36])

4.2 Light trapping by plasmonics

In the area of plasmonics, two types of surface plasmons can be generated with metallic nanostructures: localized surface plasmons (LSPs) and surface plasmon polaritons (SPPs). In case of LSPs, much smaller metal nanoparticles (tens of nanometers) efficiently scatter incident light and focus light in near-field. For SPPs, corrugated metallic films are required to convert incident light to propagation wave along the metallic film surface. Both LSPs and SPPs have been applied to CQD solar cells. Paz-Soldan et al. reported the enhanced device performance by LSPs using Au/SiO_2 nanoshells [41], as shown in Fig. 6. Beck et al. demonstrated the light trapping in CQD films by SPPs [42].

4.3 Light trapping through enhanced effective absorption length

Not only nanostructures, but large features as well can help to break the compromise between CQD film thickness and carrier extraction length. Koleilat et al. employed an architecture in CQD solar cells by folding the path of light propagating in the CQD film [43], and thus the effective absorption length in the CQD film was enhanced. Labele et al. reported the CQD solar cells with PCE as high as 9.2% using hierarchical structuring [44]. They first fabricated pyramid-shaped transparent electrodes using the stamping method. Then they conformally coated the pyramid electrodes with CQD films. As shown in Fig. 7, the pyramid structure could give more than a 2-fold improvement in effective absorption length, and lead to an overall 24% improvement in short-circuit current density.

5 Toward cost-effective CQD photovoltaics

Current CQD solar cells made in laboratories are based on solid-state ligand exchange process by spin-coating or dip-coating. This device fabrication process suffers two drawbacks: 1) Low efficiency in utilizing CQD materials – typically below 1%; 2) It is not compatible with roll-to-roll processing. This section reviews various works to develop alternative device fabrication methods for low-cost CQD photovoltaics.

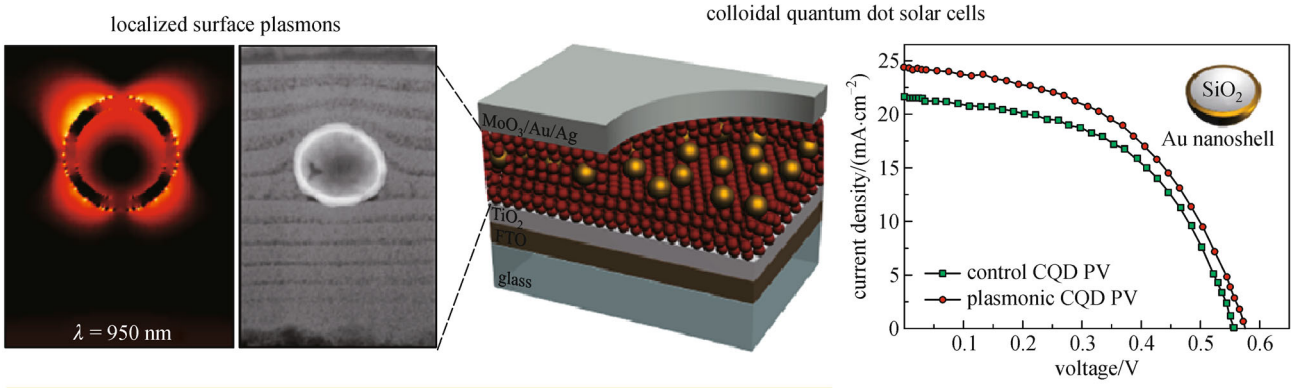

Fig. 6 Plasmonic–excitonic solar cell device design and characterization (reprinted from Ref. [41])

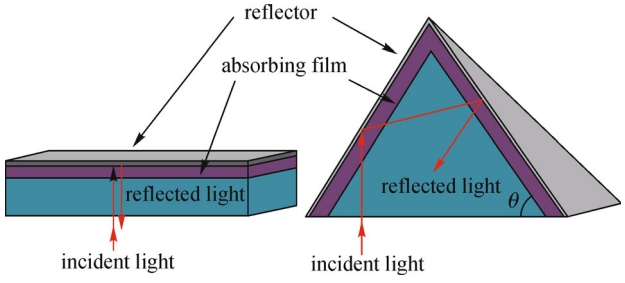

Fig. 7 Illustrating the increased-light-path advantage of pyramid-patterned electrodes (reprinted from Ref. [44])

5.1 CQD inks

In 2013, Fischer et al. developed CQD material based inks [45] for fast, serial, large-area deposition of CQD films. They replaced the solid-state ligand exchange by solution-ligand exchange. The final CQDs were encapsulated with small hydrophilic mercaptane 1-thioglycerol (TG), so that the passivation of CQD surfaces is preserved in the solution while maintaining the colloidal stability of CQDs. As a proof-of-concept, CQD solar cells using a single-step deposition were fabricated, and showed a PCE of 2.1%. This demonstration provides a compatible process to roll-to-roll printing, which represents a promising step toward cost-effect CQD solar cell manufacturing. One year later, Ning et al. pushed this work forward using halide-based ligands [46]. The finished device showed a PCE of 6% due to improved CQD passivation, as shown in Fig. 8.

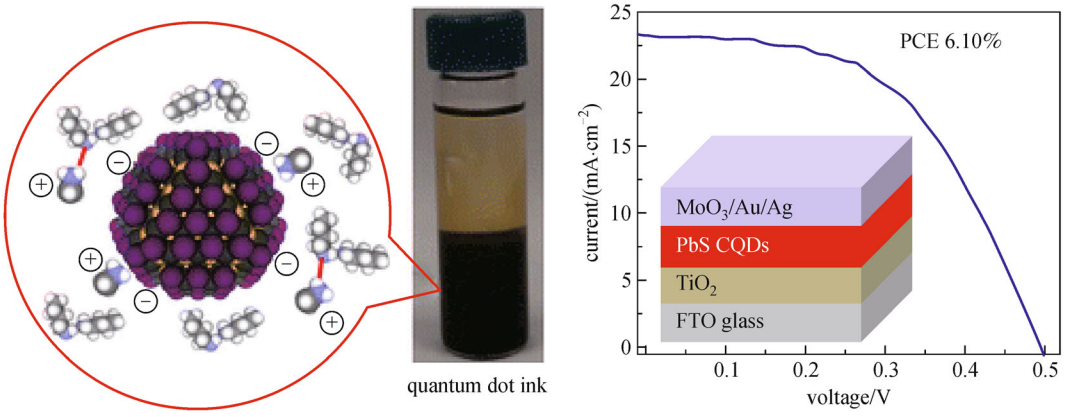

Fig. 8 n-type CQD ink based solar cells (reprinted from Ref. [46])

5.2 Spray-coated CQD solar cells

Spray-coating technique is compatible with roll-to-roll processing. Kramer et al. demonstrated the 1st spray coated CQD solar cells on rigid, curved and flexible substrates [47,48]. They achieved spray coating CQD with a fully automated process with near monolayer control, and termed this approached sprayLD. In this technique, they realized solid-state ligand exchange process using several automatically controlled fine mists, rather than spin coating. The spray-coated CQD films were dried using automatically controlled air blades, as shown in Fig. 9. The champion sprayLD device showed a PCE of 8.1% on rigid substrates. They demonstrated the potential transferability of the spray-coating technique to roll-to-roll manufacturing by spray-coating the CQD active layer onto six substrates mounted on a rapidly rotating drum.

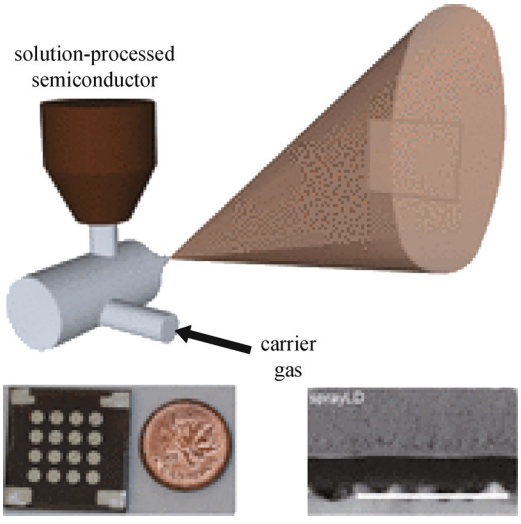

Fig. 9 Illustration of spray-coating technique and finished CQD devices (reprinted from Ref. [47])

6 Perspectives

By March 2015, the certified efficiency of CQD solar cells has reached 9.9% [49]. The understanding of device physics in CQD solar cells has been greatly extended in the past three years. Light trapping techniques have been demonstrated in CQD solar cells. Now the research community of CQD photovoltaics has theoretical and experimental tools readily available to characterize major electrical properties of CQD solar cells. It is believed that researchers will continue to improve the mobility of CQD films, identify and reduce major contribution of mid-gap traps in the near future. Initial works on CQD inks and spray coating techniques are encouraging. The demonstration of roll-to-roll manufacturing is foreseen in the next 5-10 years. As the commercialization of CQD photovoltaics is approached, more works should be started on the long-term stability of CQD solar cells.

Acknowledgements X. Wang acknowledges Prof. Jiang Tang at Wuhan National Laboratory for Optoelectronics, Huazhong University of Science and Technology, for his help and support during the manuscript preparation.

References

1. Rossetti R, Nakahara S, Brus L E. Quantum size effects in the redox potentials, resonance Raman spectra, and electronic spectra of CdS crystallites in aqueous solution. Journal of Chemical Physics, 1983, 79(2): 1086–1088
2. Murray C B, Norris D J, Bawendi M G. Synthesis and characterization of nearly monodisperse CdE (E = S, Se, Te) semiconductor nanocrystallites. Journal of the American Chemical Society, 1993, 115(19): 8706–8715
3. Shirasaki Y, Supran G J, Bawendi M G, Bulovic V. Emergence of colloidal quantum-dot light-emitting technologies. Nature Photonics, 2013, 7(1): 13–23
4. Konstantatos G, Sargent E H. Colloidal quantum dot photodetectors. Infrared Physics & Technology, 2011, 54(3): 278–282
5. Kim J Y, Voznyy O, Zhitomirsky D, Sargent E H. 25th anniversary article: colloidal quantum dot materials and devices: a quarter-century of advances. Advanced Materials, 2013, 25(36): 4986–5010
6. Kim M R, Ma D. Quantum-dot-based solar cells: recent advances, strategies, and challenges. Journal of Physical Chemistry Letters, 2015, 6(1): 85–99
7. Kramer I J, Sargent E H. The architecture of colloidal quantum dot solar cells: materials to devices. Chemical Reviews, 2014, 114(1): 863–882
8. Lan X, Masala S, Sargent E H. Charge-extraction strategies for colloidal quantum dot photovoltaics. Nature Materials, 2014, 13(3): 233–240
9. Goetzberger A, KnoblochJ, VoßB. Crystalline Silicon Solar Cells. 1st ed. New York: John Wiley & Sons Ltd, 1998, 49–86
10. Voznyy O, Thon S M, Ip A H, Sargent E H. Dynamic trap formation and elimination in colloidal quantum dots. Journal of Physical Chemistry Letters, 2013, 4(6): 987–992
11. Sze S M, Ng K K. Physics of Semiconductor Devices. 3rd ed. New York: John Wiley & Sons Ltd, 2007, 7–72
12. Ocier C R, Whitham K, Hanrath T, Robinson R D. nanocrystal field-effect transistors. Journal of Physical Chemistry C, 2014, 118(7): 3377–3385
13. Liu Y, Tolentino J, Gibbs M, Ihly R, Perkins C L, Liu Y, Crawford N, Hemminger J C, Law M. PbSe quantum dot field-effect transistors with air-stable electron mobilities above 7 $cm^2 \cdot V^{-1} \cdot s^{-1}$. Nano Letters, 2013, 13(4): 1578–1587
14. Otto T, Miller C, Tolentino J, Liu Y, Law M, Yu D. Gate-dependent carrier diffusion length in lead selenide quantum dot field-effect transistors. Nano Letters, 2013, 13(8): 3463–3469
15. Ip A H, Thon S M, Hoogland S, Voznyy O, Zhitomirsky D, Debnath R, Levina L, Rollny L R, Carey G H, Fischer A, Kemp K W, Kramer I J, Ning Z, Labelle A J, Chou K W, Amassian A, Sargent E H. Hybrid passivated colloidal quantum dot solids. Nature Nanotech-

nology, 2012, 7(9): 577–582
16. Ning Z, Ren Y, Hoogland S, Voznyy O, Levina L, Stadler P, Lan X, Zhitomirsky D, Sargent E H. All-inorganic colloidal quantum dot photovoltaics employing solution-phase halide passivation. Advanced Materials, 2012, 24(47): 6295–6299
17. Jeong K S, Tang J, Liu H, Kim J, Schaefer A W, Kemp K, Levina L, Wang X, Hoogland S, Debnath R, Brzozowski L, Sargent E H, Asbury J B. Enhanced mobility-lifetime products in PbS colloidal quantum dot photovoltaics. ACS Nano, 2012, 6(1): 89–99
18. Carey G H, Levina L, Comin R, Voznyy O, Sargent E H. Record charge carrier diffusion length in colloidal quantum dot solids via mutual dot-to-dot surface passivation. Advanced Materials, 2015, 27(21): 3325–3330
19. Zhitomirsky D, Voznyy O, Hoogland S, Sargent E H. Measuring charge carrier diffusion in coupled colloidal quantum dot solids. ACS Nano, 2013, 7(6): 5282–5290
20. Kemp K W, Wong C T O, Hoogland S H, Sargent E H. Photocurrent extraction efficiency in colloidal quantum dot photovoltaics. Applied Physics Letters, 2013, 103(21): 211101
21. Zhitomirsky D, Voznyy O, Levina L, Hoogland S, Kemp K W, Ip A H, Thon S M, Sargent E H. Engineering colloidal quantum dot solids within and beyond the mobility-invariant regime. Nature Communications, 2014, 5: 3803
22. Carey G H, Kramer I J, Kanjanaboos P, Moreno-Bautista G, Voznyy O, Rollny L, Tang J A, Hoogland S, Sargent E H. Electronically active impurities in colloidal quantum dot solids. ACS Nano, 2014, 8(11): 11763–11769
23. Tang J, Liu H, Zhitomirsky D, Hoogland S, Wang X, Furukawa M, Levina L, Sargent E H. Quantum junction solar cells. Nano Letters, 2012, 12(9): 4889–4894
24. Kemp K W, Labelle A J, Thon S M, Ip A H, Kramer I J, Hoogland S, Sargent E H. Interface recombination in depleted heterojunction photovoltaics based on colloidal quantum dots. Advanced Energy Materials, 2013, 3(7): 917–922
25. Voznyy O, Zhitomirsky D, Stadler P, Ning Z, Hoogland S, Sargent E H. A charge-orbital balance picture of doping in colloidal quantum dot solids. ACS Nano, 2012, 6(9): 8448–8455
26. Zhitomirsky D, Furukawa M, Tang J, Stadler P, Hoogland S, Voznyy O, Liu H, Sargent E H. N-type colloidal-quantum-dot solids for photovoltaics. Advanced Materials, 2012, 24(46): 6181–6185
27. Ning Z, Voznyy O, Pan J, Hoogland S, Adinolfi V, Xu J, Li M, Kirmani A R, Sun J P, Minor J, Kemp K W, Dong H, Rollny L, Labelle A, Carey G, Sutherland B, Hill I, Amassian A, Liu H, Tang J, Bakr O M, Sargent E H. Air-stable n-type colloidal quantum dot solids. Nature Materials, 2014, 13(8): 822–828
28. Stavrinadis A, Rath A K, de Arquer F P, Diedenhofen S L, Magén C, Martinez L, So D, Konstantatos G. Heterovalent cation substitutional doping for quantum dot homojunction solar cells. Nature Communications, 2013, 4: 2981
29. Ko D K, Brown P R, Bawendi M G, Bulović V. p-i-n Heterojunction solar cells with a colloidal quantum-dot absorber layer. Advanced Materials, 2014, 26(28): 4845–4850
30. Chuang C H, Brown P R, Bulović V, Bawendi M G. Improved performance and stability in quantum dot solar cells through band alignment engineering. Nature Materials, 2014, 13(8): 796–801
31. Ning Z, Zhitomirsky D, Adinolfi V, Sutherland B, Xu J, Voznyy O, Maraghechi P, Lan X, Hoogland S, Ren Y, Sargent E H. Graded doping for enhanced colloidal quantum dot photovoltaics. Advanced Materials, 2013, 25(12): 1719–1723
32. Yuan M, Zhitomirsky D, Adinolfi V, Voznyy O, Kemp K W, Ning Z, Lan X, Xu J, Kim J Y, Dong H, Sargent E H. Doping control via molecularly engineered surface ligand coordination. Advanced Materials, 2013, 25(39): 5586–5592
33. Brongersma M L, Cui Y, Fan S. Light management for photovoltaics using high-index nanostructures. Nature Materials, 2014, 13(5): 451–460
34. Kramer I J, Zhitomirsky D, Bass J D, Rice P M, Topuria T, Krupp L, Thon S M, Ip A H, Debnath R, Kim H C, Sargent E H. Ordered nanopillar structured electrodes for depleted bulk heterojunction colloidal quantum dot solar cells. Advanced Materials, 2012, 24 (17): 2315–2319
35. Lan X, Bai J, Masala S, Thon S M, Ren Y, Kramer I J, Hoogland S, Simchi A, Koleilat G I, Paz-Soldan D, Ning Z, Labelle A J, Kim J Y, Jabbour G, Sargent E H. Self-assembled, nanowire network electrodes for depleted bulk heterojunction solar cells. Advanced Materials, 2013, 25(12): 1769–1773
36. Adachi M M, Labelle A J, Thon S M, Lan X, Hoogland S, Sargent E H. Broadband solar absorption enhancement via periodic nanostructuring of electrodes. Scientific Reports, 2013, 3: 2928
37. Mahpeykar S M, Xiong Q, Wang X. Resonance-induced absorption enhancement in colloidal quantum dot solar cells using nanostructured electrodes. Optics Express, 2014, 22(S6 Suppl 6): A1576–A1588
38. Mihi A, Bernechea M, Kufer D, Konstantatos G. Coupling resonant modes of embedded dielectric microspheres in solution-processed solar cells. Advanced Optical Materials, 2013, 1(2): 139–143
39. Kim S, Kim J K, Gao J, Song J H, An H J, You T S, Lee T S, Jeong J R, Lee E S, Jeong J H, Beard M C, Jeong S. Lead sulfide nanocrystal quantum dot solar cells with trenched ZnO fabricated via nanoimprinting. ACS Applied Materials & Interfaces, 2013, 5(9): 3803–3808
40. Mihi A, Beck F J, Lasanta T, Rath A K, Konstantatos G. Imprinted electrodes for enhanced light trapping in solution processed solar cells. Advanced Materials, 2014, 26(3): 443–448
41. Paz-Soldan D, Lee A, Thon S M, Adachi M M, Dong H, Maraghechi P, Yuan M, Labelle A J, Hoogland S, Liu K, Kumacheva E, Sargent E H. Jointly tuned plasmonic-excitonic photovoltaics using nanoshells. Nano Letters, 2013, 13(4): 1502–1508
42. Beck F J, Stavrinadis A, Diedenhofen S L, Lasanta T, Konstantatos G. Surface plasmon polariton couplers for light trapping in thin-film absorbers and their application to colloidal quantum dot optoelectronics. ACS Photonics, 2014, 1(11): 1197–1205
43. Koleilat G I, Kramer I J, Wong C T O, Thon S M, Labelle A J, Hoogland S, Sargent E H. Folded-light-path colloidal quantum dot solar cells. Scientific Reports, 2013, 3: 2166
44. Labelle A J, Thon S M, Masala S, Adachi M M, Dong H, Farahani M, Ip A H, Fratalocchi A, Sargent E H. Colloidal quantum dot solar cells exploiting hierarchical structuring. Nano Letters, 2015, 15(2): 1101–1108
45. Fischer A, Rollny L, Pan J, Carey G H, Thon S M, Hoogland S, Voznyy O, Zhitomirsky D, Kim J Y, Bakr O M, Sargent E H.

Directly deposited quantum dot solids using a colloidally stable nanoparticle ink. Advanced Materials, 2013, 25(40): 5742–5749
46. Ning Z, Dong H, Zhang Q, Voznyy O, Sargent E H. Solar cells based on inks of n-type colloidal quantum dots. ACS Nano, 2014, 8 (10): 10321–10327
47. Kramer I J, Moreno-Bautista G, Minor J C, Kopilovic D, Sargent E H. Colloidal quantum dot solar cells on curved and flexible substrates. Applied Physics Letters, 2014, 105(16): 163902
48. Kramer I J, Minor J C, Moreno-Bautista G, Rollny L, Kanjanaboos P, Kopilovic D, Thon S M, Carey G H, Chou K W, Zhitomirsky D, Amassian A, Sargent E H. Efficient spray-coated colloidal quantum dot solar cells. Advanced Materials, 2015, 27(1): 116–121
49. http://www.nrel.gov/ncpv/images/efficiency_chart.jpg

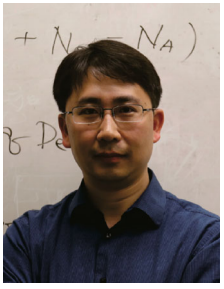

Xihua Wang received the B.Sc. degree in physics from Peking University (Beijing) in 2003, and the Master and Ph.D. degrees in physics from Boston University in 2005 and 2009, respectively. He was a Post-doctoral Fellow in the Department of Electrical and Computer Engineering at the University of Toronto from 2009 to 2012. Since July 2012, he has been an Assistant Professor in the Department of Electrical and Computer Engineering at the University of Alberta. Dr. Wang's research interests are in the area of nanomaterials and nanofabrication for photovoltaics, LEDs, photodetectors, and flexible electronics.